

A microscopic study of preferred orientation and adhesion of solid copper particles on (0001) sapphire substrates

S. T. LIN, P. D. OWNBY

Department of Ceramic Engineering, University of Missouri-Rolla, Rolla, Missouri 65401, USA

The microscopic phenomena of solid copper particles equilibrating on (0001) sapphire surfaces have been investigated by scanning electron microscopy. Very sharp and clear silhouettes of the particles are developed. At temperatures between 900 and 1080°C, with the oxygen partial pressure lower than 10^{-17} atm, the copper particles tend toward their equilibrium shape as the {111} and {110} preferred faces develop eventually into truncated octahedra or tetrakaidecahedra. Recrystallization of the particles originating at the particle-substrate interface by a heteroepitaxial mechanism is discussed. The {111} plane of the copper particles does not grow parallel to the (0001) sapphire surface as previously reported, but rather with about 20° of tilt, suggesting epitaxial growth of the Cu {112} plane on the (0001) sapphire surface. The surface energy of solid copper decreases with the increase of temperature and/or oxygen partial pressure while the work of adhesion between solid copper and (0001) sapphire can be enhanced by increasing the temperature and/or decreasing the oxygen partial pressure.

1. Introduction

Anisotropy in the surface energy of a solid body has long been recognized [1-12]. The anisotropy in the surface energy of solid metals means that a solid particle tends to form facets to reduce the system free energy, whether it is a free particle or a particle on a foreign substrate. For fcc metal solid particles resting on a solid substrate, some low index faces like the {001}, {011} and {111} have been predicted to be the largest plane faces in the equilibrium particle [1, 2]. This has been confirmed experimentally [3-9], but there are discrepancies as to the equilibrium shape of the particle.

It has also long been reported that copper heteroepitaxially grows on the (0001) sapphire surface with primarily {111} preferred orientation [3, 13, 14], even when there is a small degree of oxidation of the copper in the interface [14]. This has been attributed to the good match between {111} copper and (0001) sapphire.

With the assumptions that the effect of gravity on the shape of the particle can be neglected (valid for particles smaller than 500 μm) and that there is no appreciable chemical reaction in the solid particle-solid substrate interface, a thermodynamic calculation [10] shows that there is an equation similar to Young's equation [3, 5, 15], i.e.

$$\gamma_{sp} = \gamma_{sv} + \left(\frac{h}{H_{hkl}} \right) \gamma_{(hkl)pv} \quad (1)$$

where h is the perpendicular distance from the centre of symmetry (Wulff's point) [10] to the substrate-particle interface; H_{hkl} is the perpendicular distance

from Wulff's point to the (hkl) face; s , p and v in the subscript denote substrate, particle and vapour phase respectively; $\gamma_{(hkl)pv}$ represents the surface energy of the (hkl) face of the solid particle.

The work of adhesion of a solid metal-solid substrate system is the work required to create the new substrate and the (hkl) metal surface which were originally the common interface and is expressed as

$$W_{ad} = \gamma_{sv} + \gamma_{(hkl)pv} - \gamma_{sp} \quad (2)$$

or

$$W_{ad} = \gamma_{(hkl)pv} (1 + \cos \theta) \quad (3)$$

where θ is defined as the equivalent contact angle and is expressed as

$$\theta = 180 - \cos^{-1} \left(\frac{h}{H_{hkl}} \right) \quad (4)$$

2. Experimental procedure

The material used in this work were 99.992% pure and well polished (0001) sapphire and 99.998% pure copper wire with the major impurity being carbon (< 10 p.p.m). All the experiments were conducted in a controlled atmosphere with respect to the oxygen partial pressure (P_{O_2}) of the system, by a continuous flow of either pure dry hydrogen or a mixture of hydrogen and helium at one atmosphere total pressure. The measurement of the oxygen partial pressure was effected by a CaO stabilized ZrO₂ oxygen gauge operated at 1000°C. Lin [15] and Barsoum [16] have a detailed illustration of the experimental setup and the calculation of the oxygen partial pressure.

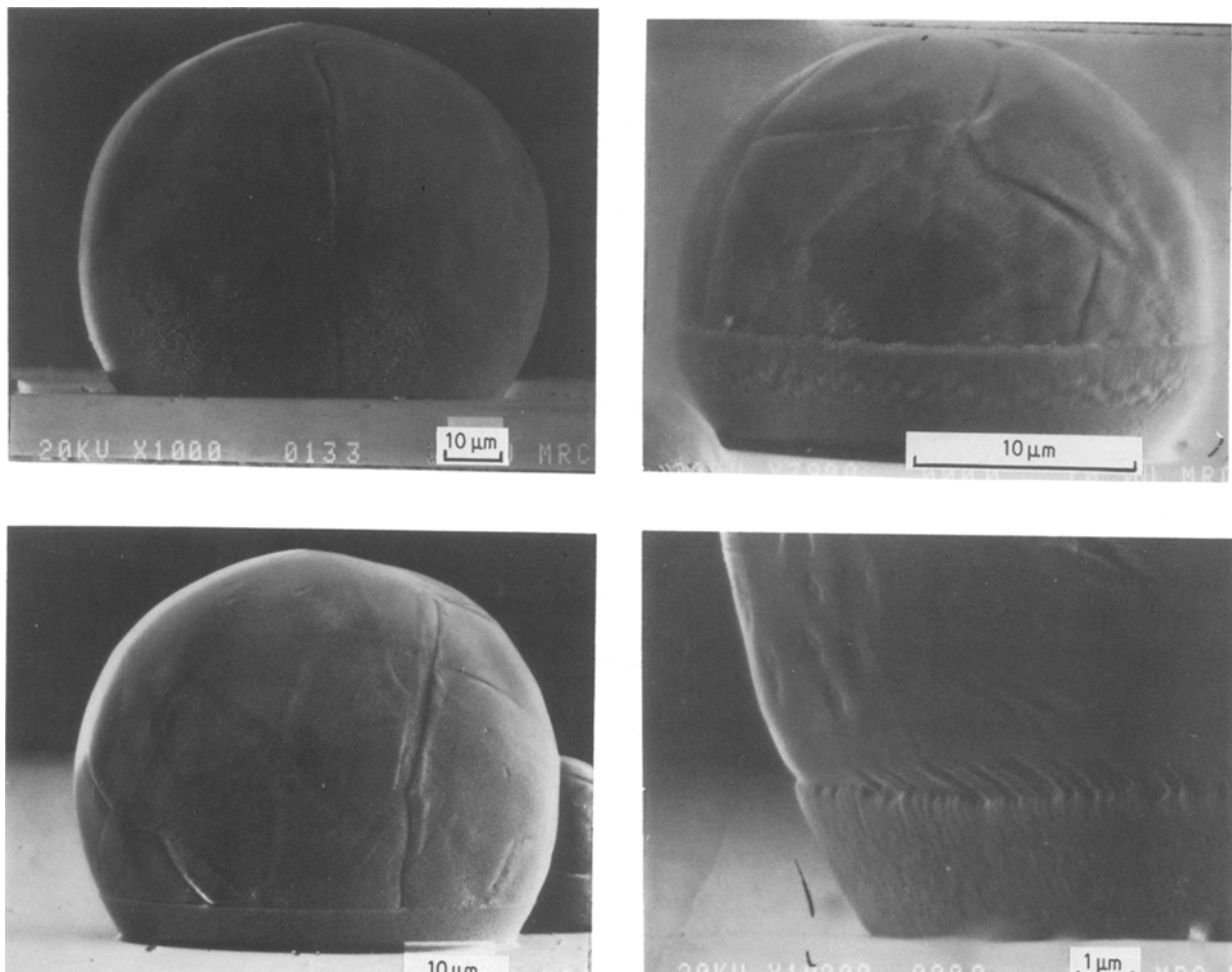


Figure 1 Crystal growth of the polycrystalline particle from the interface.

Two methods were employed to get small copper particles (1 to 100 μm) on a sapphire surface. The first was the thin wire method where a thin copper wire was put on the substrate surface and heated at 1000 $^{\circ}\text{C}$ for 2 h and then the temperature was quickly raised to 1083 $^{\circ}\text{C}$ (m.p.) to let the copper wire agglomerate and leave various sizes of small particles around the largest one. The system was then slowly cooled down to the desired temperature and kept at the temperature for about 2 days. The other was a thin film method in which a 5×10^2 nm copper film was deposited on a sapphire surface and then annealed at the desired temperature for 2 days. The criterion of 2 days has been discussed elsewhere [15]. When the specific time was reached, the system was slowly annealed to room temperature in about 14 h.

All the samples were analysed from photomicrographs taken in the scanning electron microscope (SEM).

3. Results

3.1. Crystal growth and preferred orientation

The particles formed from the thin wire method are originally polycrystalline. During annealing, the particles start to grow into single crystal particles from the particle-substrate interface. Fig. 1 clearly shows this observation.

Although taken under different environments, Figs 2 to 5 show the growth of preferred orientation

of solid copper particles on (0001) sapphire surfaces. Below each photograph is a sketch of the preferred orientation of the sample.

3.2. Anisotropy in surface energy

The anisotropy ratios of the surface energy of the non-faceted to faceted surfaces are calculated from the distances to the Wulff's point. The results at 1000 $^{\circ}\text{C}$ and $P_{\text{O}_2} = 10^{-21}$ atm (1 atm = 10^5 N m $^{-2}$)

$$\frac{\gamma_{\text{max}}}{\gamma_{111}} = 1.05 \quad (5)$$

$$\frac{\gamma_{\text{max}}}{\gamma_{100}} = 1.03 \quad (6)$$

where γ_{max} is the surface energy of the faceted surface.

3.3. Equivalent contact angle

The equivalent contact angle is calculated by Equation 4 where the values of h and H_{hkl} were not measured from the equilibrium polyhedra. Instead, they were measured from the particles before faceting because neither the edges nor the flat faces in the polyhedra really represent the average surface energy of solid copper. The surface energy of solid copper used in this work is, therefore, the average value whose magnitude is greater than that of the flat faces but smaller than that of the edges. Murr [17] has presented an argument of the validity of this approach. The variation of $\cos \theta$ with temperature is shown in Fig. 6.

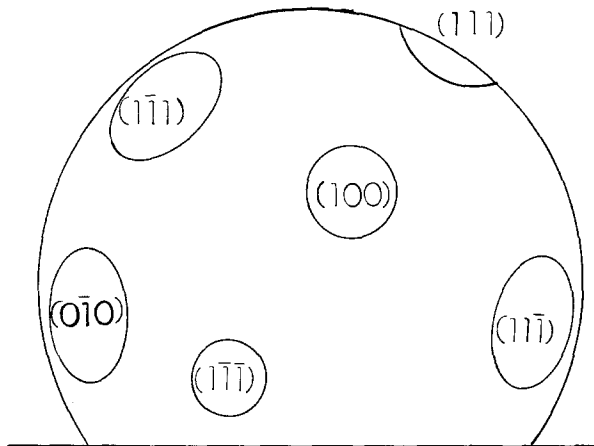
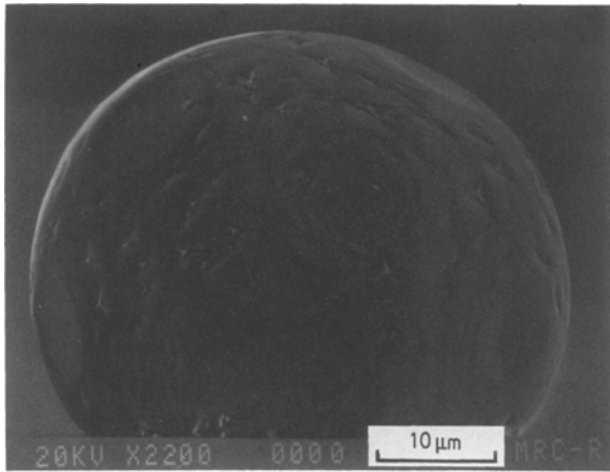


Figure 2 The growth of preferred orientation (1), $P_{O_2} = 3 \times 10^{-21}$ atm, 1040°C for 52 h.

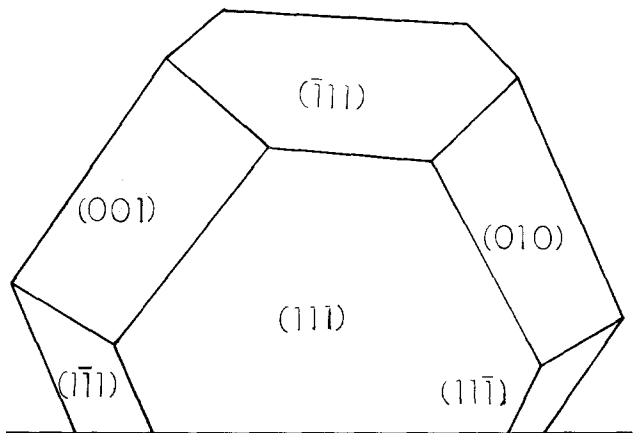
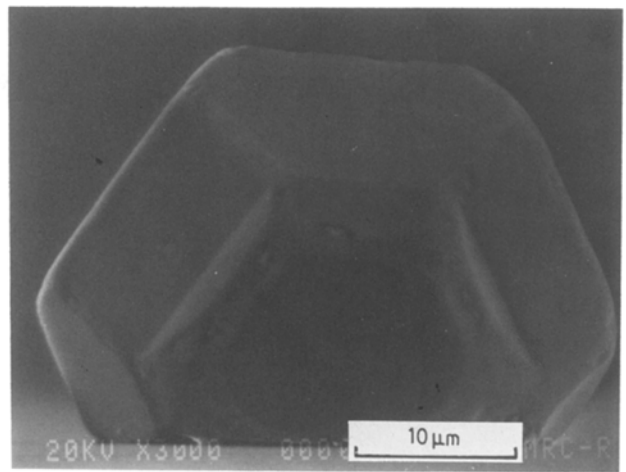


Figure 4 The growth of preferred orientation (3), $P_{O_2} = 4 \times 10^{-21}$ atm, 1040°C for 52 h.

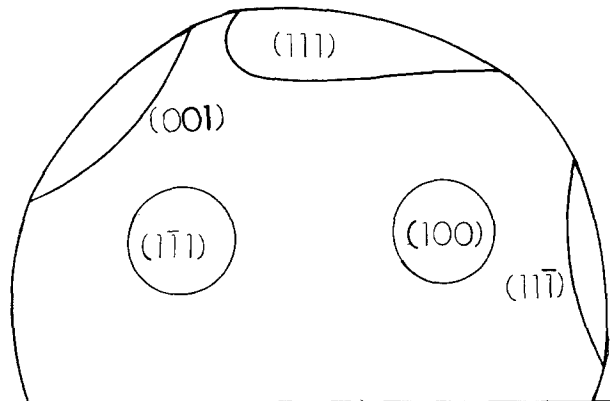
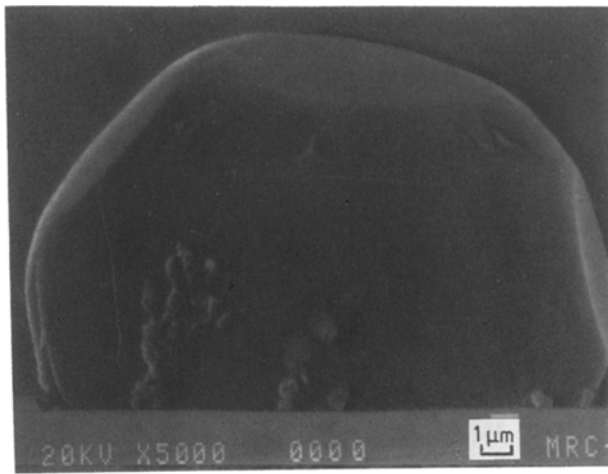


Figure 3 The growth of preferred orientation (2), $P_{O_2} = 4 \times 10^{-21}$ atm, 1000°C for 50 h.

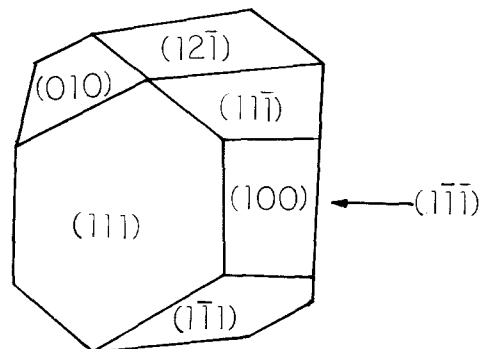
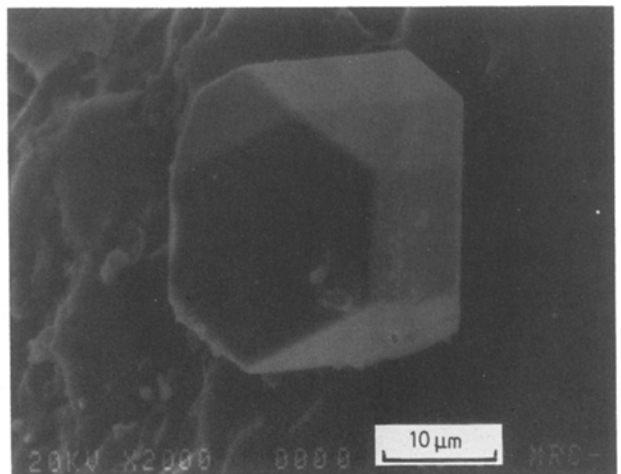


Figure 5 The growth of preferred orientation (4), $P_{O_2} = 2 \times 10^{-23}$ atm, 960°C for 27 h, thin film method, top view.

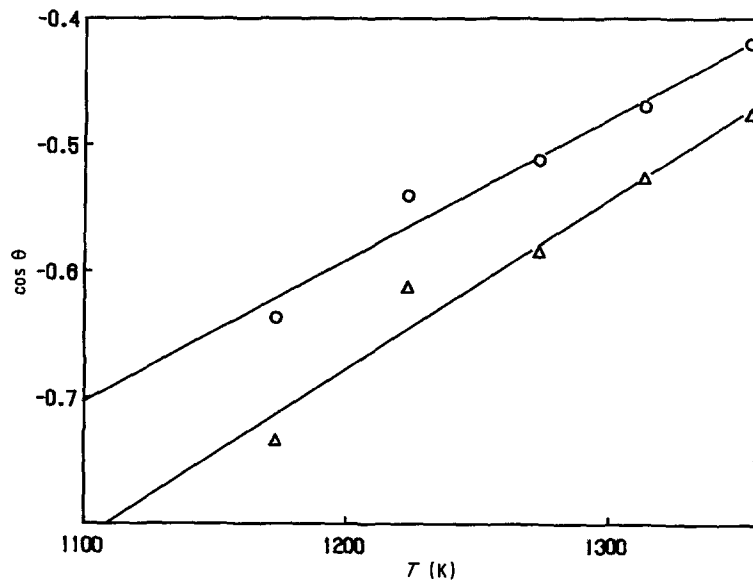


Figure 6 The variation of $\cos \theta$ with temperature. (\circ 10^{-21} atm, Δ 10^{-17} atm).

3.4. Interfacial energy and work of adhesion

The surface energy of sapphire used in this study is based on the equation measured by Nikolopoulos [18] and is assumed to be little affected by the oxygen partial pressure in the range from 10^{-21} atm to 10^{-17} atm

$$\gamma_{sv}(\text{Al}_2\text{O}_3) = 2.559 - 7.84 \times 10^{-4} T \text{ (J m}^{-2}\text{) (K)} \quad (7)$$

The surface energy of solid copper in $P_{\text{O}_2} = 10^{-21}$ atm is assumed to be equivalent to the measurement by Udin [19] at a vacuum of 10^{-5} torr

$$\gamma_{pv}(\text{Cu}) = 2.396 - 5.5 \times 10^{-4} T \text{ (J m}^{-2}\text{) (K)} \quad (8)$$

Lin [15] has discussed the reasons for choosing these two equations.

Because the copper-sapphire interface is not exposed to the environmental gas, the interfacial energy of copper-sapphire was assumed to be constant in the oxygen partial pressure range between 10^{-21} atm and 10^{-17} atm so that the surface energy of solid copper can be correlated with oxygen partial pressure as well as temperature. The variation of copper surface

energy, the copper-sapphire interfacial energy and the work of adhesion with temperature are shown in Figs 7, 8 and 9, respectively. Linear regressions of the data sets at temperatures between 1173 and 2353 K give the following expressions

$$(1) P_{\text{O}_2} = 10^{-21} \text{ atm}$$

$$\gamma_{sp}(\text{Cu} - (0001) \text{ sapphire}) = 6.1934 - 2.96 \times 10^{-3} T \text{ (J m}^{-2}\text{) (K)} \quad (9)$$

$$W_{ad}(\text{Cu} - (0001) \text{ sapphire}) = -1.2712 + 1.65 \times 10^{-3} T \text{ (J m}^{-2}\text{) (K)} \quad (10)$$

$$(2) P_{\text{O}_2} = 10^{-17} \text{ atm}$$

$$\gamma_{pv}(\text{Cu}) = 1.8672 - 3.0 \times 10^{-4} T \text{ (J m}^{-2}\text{) (K)} \quad (11)$$

$$W_{ad}(\text{Cu} - (0001) \text{ sapphire}) = -1.7712 + 1.88 \times 10^{-3} T \text{ (J m}^{-2}\text{) (K)} \quad (12)$$

4. Discussion

It is readily seen from the SEM pictures that the particle, before it develops its equilibrium faceted

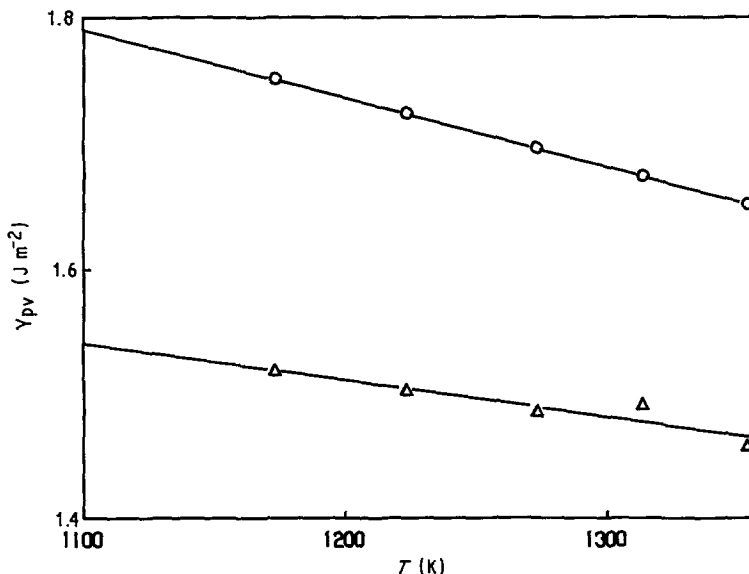


Figure 7 The variation of surface energy of copper, γ_{pv} , with temperature (\circ 10^{-21} atm, Δ 10^{-17} atm).

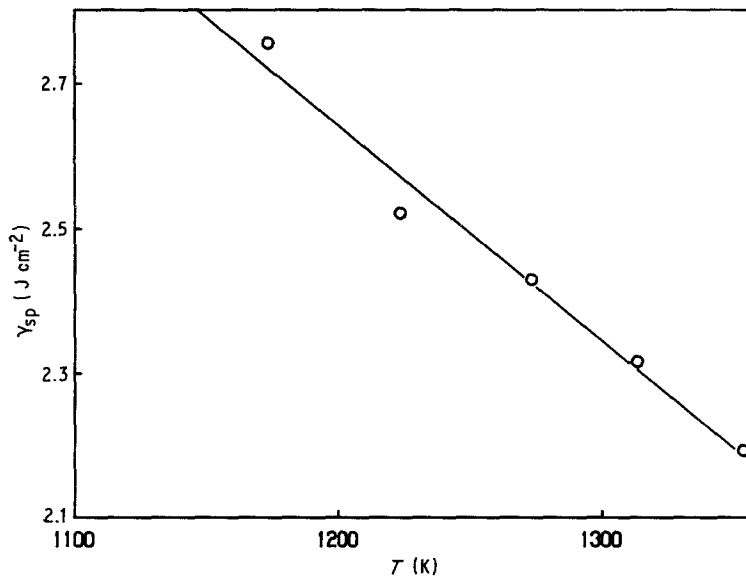


Figure 8 The variation of interfacial energy, γ_{sp} , with temperature.

shape, has the approximate shape of a truncated sphere. Calculation [15] shows that upon solidification and annealing from 1083°C to 25°C there is a small degree of linear thermal contraction on each side of the particle (<1.5%). It is also observed that the equivalent contact angle calculated by Equation 4 is always greater than the directly measured one by less than 5°, a phenomenon that is quite reasonable since there is some degree of wetting of copper on sapphire so that the copper near the contact plane shows a smaller degree of thermal contraction.

Previous studies have involved either sharp faceted particles with a large angle of tilt in SEM because of the technical difficulty in obtaining photomicrographs of dense particles with a small angle of tilt [5–8], or submicrometre particles in other reports [3, 4, 9, 10, 17, 20–22], where the proposed models of the equilibrium particle shape were based on a two-dimensional top view observation. One important aspect of this study is that sharp and clear silhouettes of particles with a size of tens of micrometres are observed at less than 8° of tilt from the horizontal in the SEM.

4.1. Crystal growth of particle

The recrystallization of the polycrystalline copper particles starts from the copper–sapphire interface

and grows parallel to the interface. This phenomenon has been previously reported [7]. This process can be attributed to bulk volume self-diffusion, perpendicular to the interface, a phenomenon also observed before [8].

Grain boundaries contribute excess free energy, \bar{G} in a polycrystalline particle, whose effect is a driving force for recrystallization. Ignoring the effects of grain straining and the difference in the free energy between grain orientations, the driving force for the hetero-epitaxial recrystallization from the particle–substrate interface by thermal annealing, is totally determined by the grain boundary energy.

For an ideal polycrystalline particle originally with only two grains of equal volume and a flat grain boundary perpendicular to the particle–substrate interface as shown in Fig. 10, the excess free energy can be calculated from the area of grain boundary and is expressed as

$$\begin{aligned} \bar{G} = & \gamma_{gb} r^2 \left(\pi - \pi [\cos \theta + (w/r)]^2 \right. \\ & + \frac{\cos^{-1} [\cos \theta + (w/r)]}{180} \pi - [\cos \theta + (w/r)] \\ & \left. \times \{1 - [\cos \theta + (w/r)]\}^{1/2} \right) \end{aligned} \quad (13)$$

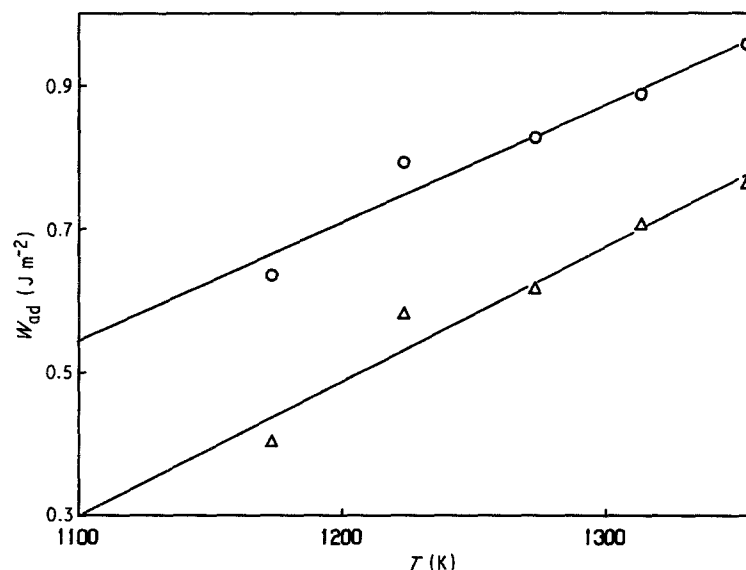


Figure 9 The variation of work of adhesion, W_{ad} , with temperature (O 10^{-21} atm, Δ 10^{-17} atm).

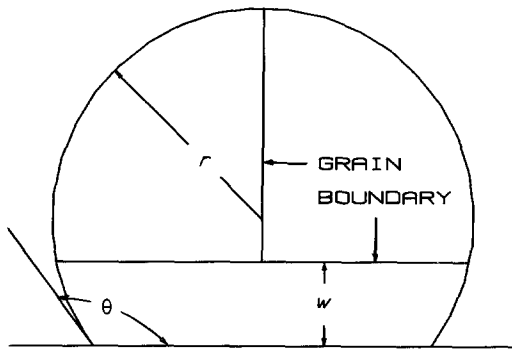


Figure 10 An ideal model of the recrystallization from a bicrystal particle.

where γ_{gb} represents the grain boundary energy. The variation of excess free energy with respect to the dimensionless width of the heteroepitaxial growth layer, (w/r), is shown in Fig. 11. From this figure it is readily seen that stable growth of this layer must be preceded by a nucleation step which overcomes the activation energy, E_a , and then the system free energy of the particle decreases to a minimum as the epitaxial layer grows to the top of the particle and disappears.

The variation of the relative magnitude of the activation energy, which is proportional to the grain boundary energy and surface area of the particle, with the contact angle shown in Fig. 12. Therefore, the contact angle as well as the other factors like particle size, grain boundary energy, annealing temperature and annealing time, is an important factor in the recrystallization of the particle.

4.2. Preferred orientation

A final equilibrium shape of a truncated octahedron or tetrakaidecahedron, is proposed for a model of the particle shape (Fig. 13). This crystal form has $m\bar{3}m$ point group symmetry with four three-fold rotational axes and two mirror planes [23].

In the growth of preferred orientations, some low index faces ($\{100\}$, $\{110\}$, $\{111\}$, $\{112\}$ etc.) first develop and later $\{111\}$ and $\{100\}$ predominate at the expense of the other faces, a phenomenon that has been explained by the fast growth as well as the thermodynamic instability of these disappearing

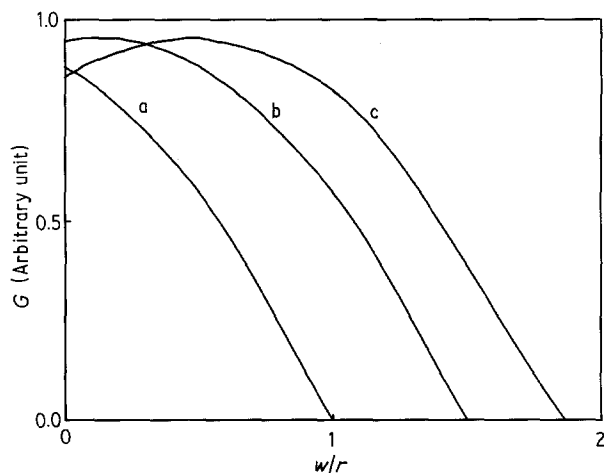


Figure 11 The variation of excess free energy with the dimensionless thickness of the growth layer (a $\theta = 90^\circ$, b $\theta = 120^\circ$, c $\theta = 150^\circ$).

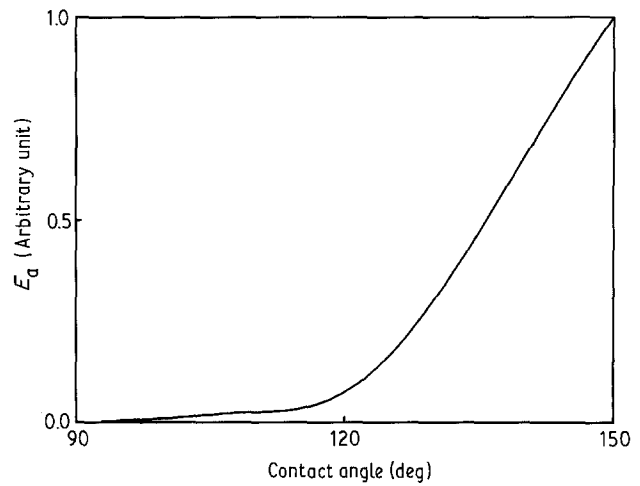


Figure 12 The variation of the relative magnitude of activation energy with contact angle.

faces [8]. The mechanism of sphere faceting by surface self-diffusion [6] is evident because multiple rings are observed around the particle facets before the equilibrium shape is attained. Fig. 14 shows a two-dimensional drawing of the facet growth of a particle by surface self-diffusion.

At least in the temperature range of 900 to 1083°C with $P_{O_2} < 10^{-17}$ atm, no appreciable $\{110\}$ faces are observed in the equilibrium shape and the maximum anisotropy in surface energy of copper is, within the experimental sensitivity, smaller than 5%, a result similar to that of Mclean *et al.* [11].

One important observation that has to be pointed out here is that almost every former investigator [3, 9, 13] directly or indirectly observed and reported that $\{111\}$ copper heteroepitaxially grows on (0001) sapphire surface. The X-ray diffraction pattern of one sample in this work (Fig. 15) does show a preferred Cu $\{111\}$ orientation on the sapphire substrate. From Figs 2 to 5, it is seen that $\{111\}$ face is not really parallel to the (0001) sapphire surface, but rather off parallel by about 20° of tilt. One previous observation reported a 6.5° tilt [14]. The value of 20° of tilt can be seen from the photomicrograph of Fig. 5, where the $\{111\}$ face indicated by an arrow is almost perpendicular to the substrate surface. The interplanar angle between the $\{111\}$ family of planes is 70.5° so that the $\{111\}$ plane of the large hexagon in the figure is about 19.5° of tilt from the substrate surface. The most

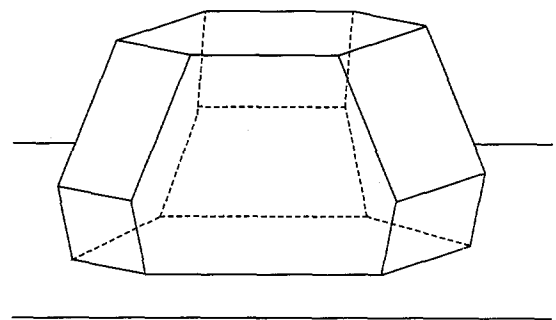


Figure 13 The truncated octahedron (tetrakaidecahedron) with $\{111\}$ and $\{100\}$ preferred orientation, hexagons- $\{111\}$, squares- $\{100\}$.

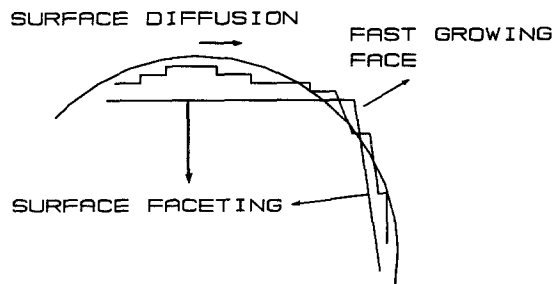


Figure 14 The mechanism of the facet growth of the particle by surface diffusion.

probable candidate for this epitaxial plane is the $\{112\}$ plane since the interplanar angle between the $\{100\}$ plane and $\{112\}$ plane is 19.5° and, as mentioned above, this thermodynamically unstable low index face is the fast growing face.

4.3. Magnitude of error

The sources of error are primarily the uncertainty in measuring the linear dimensions of h and H , the tilt angle of substrate in SEM photomicrographs, and those arising from the migration of impurities to the surface of the copper particles. The error associated with these three factors is about 3° of uncertainty in the values of equivalent contact angle [15].

4.4. Effect of oxygen partial pressure

The surface of the copper particles become rougher as the oxygen partial pressure increases from 10^{-21} atm to 10^{-17} atm, a phenomenon that can be attributed to the surface adsorption or oxidation of solid copper, because although this is below the equilibrium oxygen partial pressure for oxide formation at the experimental temperature, where it has been reported to be an 0.24 monolayer coverage in $P_{O_2} = 10^{-17}$ atm [24], the photomicrographs were taken after cooling to room temperature where the equilibrium oxygen partial pressure was certainly exceeded.

The effect of oxygen partial pressure on the work of adhesion of a solid copper-sapphire substrate system is contrary to that of a liquid copper-sapphire substrate system [25-27]. This can be ascribed to the earlier assumption that the interfacial energy of the solid copper-sapphire substrate is not as seriously affected by the increase of oxygen partial pressure as the surface energy of solid copper. The decrease of the surface energy of solid copper results, in effect, in the de-wetting of the system.

Extrapolation of the surface energy of solid copper in $P_{O_2} = 10^{-17}$ atm to the melting point (1356 K) gives a value of 1.460 J m^{-2} . This result is very consistent with the rule of approximately 10% increase upon solidification for the surface energy of metals [28], since most of the reported data of the surface energy of liquid copper at its melting point is in the range 1.300 to 1.400 J m^{-2} in $P_{O_2} = 10^{-16}$ atm [25-27].

The transition oxygen partial pressure, which is defined as the commencing oxygen partial pressure of the Gibb's adsorption isotherm (a linear section in the plot of the surface energy with $\log P_{O_2}$), is reported to be 10^{-23} atm at 1200 K [29], 10^{-21} atm at 1300 K [24], and 10^{-16} atm at 1356 K (liquid phase) [25-27].

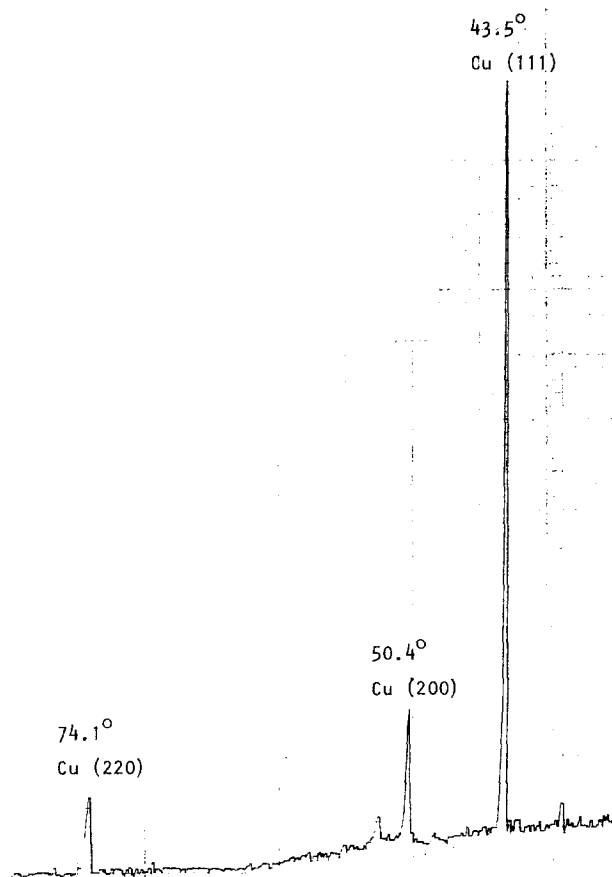


Figure 15 X-ray diffraction pattern of solid copper particle on (0001) sapphire surface. 500 nm copper film 1060°C for 55 h. $P_{O_2} = 2 \times 10^{-20}$ atm.

Although the surface energies of solid copper reported by Mclean *et al.* [29] and Sauer *et al.* [24] are very small and even smaller than that of liquid copper [25-27], the differences in the surface energy of copper in $P_{O_2} = 10^{-21}$ atm and $P_{O_2} = 10^{-17}$ atm are about 0.300 J m^{-2} at 1200 K [29] and 0.400 J m^{-2} at 1300 K [24] while the difference in this study is 0.190 J m^{-2} . This is quite reasonable since the $P_{O_2} = 10^{-21}$ atm in this study is smaller than the transitional oxygen partial pressure at 1356 K.

5. Conclusions

This study has explored the microscopic behaviour of small solid copper particles equilibrating on (0001) sapphire substrates in the temperature range $1173 < T < 1352 \text{ K}$ and oxygen partial pressure range 10^{-21} atm and 10^{-17} atm.

The polycrystalline copper particles heteroepitaxially grow on the substrate surface from the particle-substrate interface by bulk volume self-diffusion. The copper particle tends to develop so that the exposed faces are low index faces of $\{111\}$ and $\{100\}$ preferred orientations by surface self-diffusion. The sharp and clear equilibrium shape of truncated octahedra is observed. The maximum anisotropy in the surface energy of solid copper is calculated to be less than 5%. From all the photomicrographs taken, it is obvious that the $\{111\}$ face of the copper particle does not really grow parallel to the (0001) sapphire surface, but rather with about 20° of tilt. The probable epitaxial

growth plane is reasoned to be Cu {112} || Sapphire (0001).

The work of adhesion between solid copper and the (0001) sapphire surface increases with the increase in temperature. An increase in oxygen partial pressure from 10^{-21} atm to 10^{-17} atm causes the decrease in the surface energy of solid copper and therefore partly accounts for the decrease in work of adhesion of the system.

References

1. M. DRECHSLER, in "Surface Mobility on Solid Materials", edited by V. T. Binh (Plenum, New York, 1981) p. 405.
2. M. McLEAN and E. K. HONDROS, *ibid.*, p. 459.
3. R. M. PILLER and J. NUTTING, *Phil. Mag.* **16** (1967) 181.
4. T. WANG, C. LEE and L. D. SCHMIDT, *Surf. Sci.* **163** (1985) 181.
5. J. C. HEYRAUD and J. J. METOIS, *J. Cryst. Growth* **50** (1980) 571.
6. J. J. METOIS and J. C. HEYRAUD, *ibid.* **57** (1982) 487.
7. J. J. METOIS, G. D. T. SPILLER and J. A. VENABLES, *Phil. Mag.* **46A** (1982) 1015.
8. T. C. CHOU and Y. T. CHOU, *J. Mater. Sci. Lett.* **4** (1985) 1340.
9. B. E. SUNDQUIST, *Acta Metall.* **12** (1964) 67.
10. W. L. WINTERBOTTOM, *Acta Metall.* **15** (1967) 303.
11. M. McLEAN and B. GALE, *Phil. Mag.* **20** (1969) 1933.
12. R. S. NELSON, D. J. MAZEY and R. S. BARNES, *Phil. Mag.* **11** (1965) 91.
13. G. KATZ, *Thin Solid Films* **33** (1976) 99.
14. W. LISHI, J. HAAG and G. PETZOW, in "Microstructure and Properties of Ceramic Materials", edited by T. S. Yen and J. A. Pask (Science Press and Elsevier Publisher, Shanghai, 1984) p. 125.
15. S. T. LIN, MS Thesis, University of Missouri - Rolla, Rolla, Missouri (1987).
16. M. BARSOUM, MS Thesis, University of Missouri - Rolla, Rolla, Missouri (1980).
17. L. E. MURR, in "Adhesion Measurement of Thin Films, Thick Films, and Bulk Coatings", edited by K. L. Mittal (American Society for Testing and Materials, Philadelphia, 1978) p. 82.
18. P. NIKOLOPOULOS, *J. Mater. Sci.* **20** (1985) 3993.
19. H. UDIN, *J. Metal.* **189** (1951) 63.
20. L. E. MURR, *Mater. Sci. Eng.* **12** (1973) 277.
21. L. E. MURR and U. M. AHMAD, *Scripta Metall.* **10** (1976) 299.
22. L. E. MURR, in "Surfaces and Interfaces in Ceramic and Ceramic Metal Systems", edited by J. Pask and A. Evans (Plenum, New York, 1980) p. 107.
23. L. H. SCHWARTZ and J. B. COHEN, in "Diffraction from Materials" (Academic, New York, 1977) p. 39.
24. C. E. BAUER, R. SPEISER and J. P. HIRTH, *Met. Trans.* **7A** (1976) 75.
25. S. P. MEHROTRA and A. C. D. CHAKLADER, *ibid.* **16B** (1985) 567.
26. B. GALLOIS and C. H. LUPIS, *ibid.* **12B** (1981) 549.
27. J. LIU, MS Thesis, University of Missouri - Rolla, Rolla, Missouri (1987).
28. A. S. SKAPSKI, *Acta Metall.* **4** (1956) 576.
29. M. McLEAN and E. D. HONDROS, *J. Mater. Sci.* **8** (1973) 349.

Received 11 August
and accepted 1 December 1987